*Published online 14 October 2020*

*Nucleic Acids Research, 2020, Vol. 48, No. 20* ***e115***
*doi: 10.1093/nar/gkaa833*

# Efficient DNA double-strand break formation at single or multiple defined sites in the *Saccharomyces cerevisiae* genome

**Robert Gnügge [1,*] and Lorraine S. Symington [1,2]**

[1]Department of Microbiology & Immunology, Columbia University Irving Medical Center, New York, NY 10032, USA and [2]Department of Genetics & Development, Columbia University Irving Medical Center, New York, NY 10032, USA

Received March 28, 2020; Revised August 18, 2020; Editorial Decision September 16, 2020; Accepted September 28, 2020

## ABSTRACT

**DNA double-strand breaks (DSBs) are common genome lesions that threaten genome stability and cell survival. Cells use sophisticated repair machineries to detect and heal DSBs. To study DSB repair pathways and associated factors, inducible site-specific endonucleases have proven to be fundamental tools. In *Saccharomyces cerevisiae*, galactose-inducible rare-cutting endonucleases are commonly used to create a single DSB at a unique cleavage site. Galactose induction requires cell cultivation in sub-optimal growth media, which is tedious especially when working with slow growing DSB repair mutants. Moreover, endonucleases that simultaneously create DSBs in multiple defined and unique loci of the yeast genome are not available, hindering studies of DSB repair in different genomic regions and chromatin contexts. Here, we present new tools to overcome these limitations. We employ a heterologous media-independent induction system to express the yeast HO endonuclease or bacterial restriction enzymes for single or multiple DSB formation, respectively. The systems facilitate tightly controlled and efficient DSB formation at defined genomic sites and will be valuable tools to study DSB repair at a local and genome-wide scale.**

## INTRODUCTION

The genome of a cell is constantly damaged (1). Endogenous metabolites, such as reactive oxygen species, and cell inherent processes, such as replication, can damage the cell's DNA. In addition, DNA damage arises when the cell is exposed to harmful chemicals and irradiation. DNA double-strand breaks (DSBs) are particularly dangerous forms of damage, which threaten genome integrity and cell survival (2). Despite their harmful nature, cells also actively generate DSBs during programmed processes, such as meiosis and lymphocyte development (3,4). Moreover, many genome editing technologies rely on controlled DSB formation (5). Cells use sophisticated mechanisms to detect and repair DSBs (6). Mutated DSB repair factors are associated with cancer-prone syndromes and developmental, neurological, and immunological diseases (7). On the other hand, the DSB repair deficiency of cancer cells can be exploited using DSB-generating drugs and irradiation as treatments. Thus, a better understanding of DSB repair and its regulation remains an important goal in basic, applied, and biomedical research.

We owe much of our current understanding of DSB repair to experiments using site-specific endonucleases to efficiently create DSBs at defined genome loci in live cells. Endonuclease-mediated DSB formation has been the basis for many genetic, biochemical, and cell-biological assays that helped define different DSB repair pathways and the contribution and interplay of repair factors (8–12).

In the budding yeast *Saccharomyces cerevisiae*, the endonuclease HO is widely used for site-specific DSB formation. HO is a yeast-endogenous enzyme, which initiates mating type switching by creating a DSB at the *MAT* mating type locus (13). Recombination with one of two transcriptionally silent repair cassettes (*HML* and *HMR*) replaces coding sequences at the *MAT* locus and switches the mating type. For DSB repair studies, an HO gene under the control of the *GAL10* promoter (*GAL-HO*) is commonly used (14), as it allows galactose-inducible synchronous DSB formation at the endogenous *MAT* locus or engineered recognition sequences in a cell population.

A shortcoming of the *GAL-HO* system is its requirement for specific nutrient conditions (15). For efficient galactose-induction, cells need to be precultured with a non-fermentable carbon source, which slows down cell growth. This is especially cumbersome when working with mutants conferring a cell growth defect and many DSB repair mutants show this phenotype. Mutations in the glucose repression pathway can alleviate this shortcoming (16). However, the mutations themselves reduce cell growth

*To whom correspondence should be addressed. Robert Gnügge. Tel: +1 212 305 7753; Fax: +1 212 305 1468; Email: robert.gnuegge@gmail.com

and cause general metabolic, cell biological, and signaling defects (17,18). The nutrient requirements of galactose-induction also limit the metabolic states in which DSB signaling and repair can be studied.

Here, we use a heterologous induction system to control HO expression. We show that this new system is media-independent, tightly controlled, and leads to the efficient formation of a single DSB in the yeast genome.

DSB formation at a unique site in the genome is appropriate for various experimental settings. For example, such systems allow the genetic requirements for DSB repair to be studied (12,19–21). However, if DSB repair in different genome regions and chromatin contexts is to be analyzed, synchronous DSB formation at multiple defined genomic sites is desirable.

One way to generate multiple DSBs is to increase the number of endonuclease recognition sites in the genome. In case of the HO endonuclease, the yeast genome contains three recognition sites, which are located at the *MAT* locus and at the *HML* and *HMR* repair cassettes (13). The transcriptionally silenced state of the repair cassettes prevents their cleavage, such that HO expression leads to DSB formation only at *MAT*. If the repair cassettes are unsilenced by mutations in the silencer complex, all three recognition sites are accessible to HO and three defined DSBs can be generated (21). A shortcoming of this approach is that the sequences around the DSBs at *MAT* and one of the cassettes are identical. Moreover, inactivating the silencer complex unsilences additional genomic regions, such as subtelomeric sequences (22). As an alternative approach, synthetic HO cleavage sites can be inserted at defined genomic loci (23). However, inserting multiple cleavages sites is tedious and propagating them through strain crossings is inefficient. Several HO cut sites have been inserted into the yeast genome using an inducible retrotransposon carrying a selectable marker and an HO cleavage site (24). A limitation of this system is that the insertion sites cannot be controlled and that all HO cut sites are embedded in identical *Ty1* yeast transposon sequences. Moreover, their cutting efficiency is reduced compared to the endogenous *MAT* HO cleavage site.

An alternative approach to inserting multiple cleavage sites is to use endonucleases whose recognition sequences naturally occur at multiple loci in the yeast genome. Available systems employ the bacterial restriction enzymes EcoRI, EcoRV, or PvuII under the control of galactose-inducible promoters (25–27). These systems were used to study the requirement of repair factors in different repair pathways and DSB signaling. However, the 6 bp long recognition sequences of the employed restriction enzymes occur at several thousand loci in the yeast genome. The high number of DSBs may result in unphysiological recognition and processing of the breaks due to low repair factor recruitment to each of them and exhaustion of the repair machinery. Moreover, the recognition sequences also occur in repetitive and high-copy sequences, such as ribosomal DNA, mitochondrial DNA, yeast transposons, and the 2 micron plasmid, preventing unambiguous mapping of the corresponding DSBs.

Here, we generate multiple defined DSBs using bacterial restriction enzymes whose 8 bp long recognition sequences occur naturally at ca. 20–100 unique, non-repetitive loci in the yeast genome. We controlled expression of the restriction enzymes with a heterologous induction system to achieve media-independent, tightly regulated, and efficient DSB formation.

## MATERIALS AND METHODS

### Plasmids

Supplementary Table S1 lists all plasmids used in this work. Plasmid sequences were confirmed by control digests and Sanger sequencing (Genewiz).

The plasmids containing the *lexO-HO* system were cloned in two steps. First, the $P_{lexO}$-*HO*-$T_{CYC1}$ gene was cloned into pRG205MX (28) by fusing the SacI–SpeI $P_{lexO}$ fragment of FRP1671 (28) to the EcoRI-XhoI cloned *HO* coding sequence amplified from pSD160 (29) and XhoI–KpnI cloned $T_{CYC1}$ amplified from *S. cerevisiae* S288C genomic DNA. The complete insert was then excised with EagI and inserted into the NotI site of pRG203MX, pRG205MX, or pRG206MX (28) containing the $P_{ACT1}$-*LexA-ER-B112*-$T_{CYC1}$ SacI–KpnI fragment from FRP880 (30).

The protein sequences of AsiSI, AscI, FseI, and SbfI were derived from UniProt (accession numbers: Q83XX1, E3VXA3, F1KC51, Q4TZJ3). The protein sequence of SrfI was kindly provided by New England Biolabs. Protein sequences were appended with the PKKKRKV nuclear localization signal and the DYKDDDDK FLAG tag, codon optimized for expression in *S. cerevisiae*, acquired as GeneArt® Strings DNA Fragments (Thermo Fisher Scientific), and cloned as EcoRI–XhoI fragments. Plasmids containing both the inducible restriction enzyme genes and the LexA-ER-B112 transcription factor were then cloned in the same way as the *lexO-HO* system (see above).

The Cas9 plasmid targeting the *MAT*a HO cut site was derived from the pCAS plasmid (31) and contained the sequence TTTATAAAATTATACTGTTG for targeting.

For the single-strand annealing (SSA) assay, we cloned a cassette to replace the *MAT*a HO cut site region. The SSA cassette was assembled from several parts in pBluescript (Stratagene, USA). Targeting sequence H1 corresponds to the sequence stretch located 259 bp to 25 bp upstream of the *MAT*a HO cut site and was cloned as a SacI/AscI–XbaI fragment from *S. cerevisiae* W303 genomic DNA. Targeting sequence H2 corresponds to the sequence stretch located 25 bp to 236 bp downstream of the *MAT*a HO cut site and was cloned as a XhoI–AscI/KpnI fragment from *S. cerevisiae* W303 genomic DNA. The *URA3MX-Δ3* and *URA3MX-Δ5* parts were cloned as XbaI–BamHI and HindIII–XhoI fragments from pRG206MX (28), respectively. The *HIS3MX* marker was cloned as a EcoRI–HindIII fragment from pRG203MX (28). The 50 bp centered on the *MAT*a HO cut site were derived as oligonucleotides with BamHI and EcoRI overhangs, annealed, and cloned into the center of the cassette.

### Yeast strains

Supplementary Table S2 lists all yeast strains used in this work. Strains were generated by crossing or by

transformation with AscI-linearized plasmids using the Lithium acetate method (32). Integration of plasmids with pRG203MX, pRG205MX, or pRG206MX backbone was confirmed by colony PCR as previously described (28). Integration of the SSA cassette was confirmed by colony PCR with oRG167+oRG301 and oRG168+oRG302 (Supplementary Table S3). *BAR1* was deleted by one-step gene replacement using a PCR-derived *hphMX* cassette (33).

The AsiSI, AscI, FseI, SbfI, or SrfI recognition sequence was inserted into the *MAT*a HO cut site by Cas9-mediated genome engineering using the method described in (31). The repair templates were generated by assembly PCR using oRG161+oRG164 as external primers and oRG162+oRG163, oRG205+oRG206, oRG207+oRG208, oRG2011+oRG212, or oRG213+oRG214 as internal primers (Supplementary Table S3). The genome modifications were confirmed by PCR amplification with oRG167+oRG168 and Sanger sequencing.

### Yeast media and culture conditions

Complex yeast medium contained 1% yeast extract, 2% peptone, and 2% glucose (YPD), 2% lactate (YPL), 2% galactose (YPG), or 2% lactate and 2% galactose (YPLG). Synthetic yeast media contained 1× YNB, 1× amino acid mix lacking specific amino acids and 2% glucose (SD) or 2% raffinose (SR). Solid media additionally contained 2% agar.

Yeast cells were grown at 30°C. Liquid cultures were shaken vigorously.

### DSB quantification by quantitative PCR (qPCR)

DSB quantification by qPCR was performed as described previously (34). Briefly, cells were grown in non-inducing conditions; cells containing *GAL-HO* were grown in YPL, while cells containing the *lexO-HO* system were grown in YPD, YPL, YPLG, or SD-Leu. G1-cell cycle arrest was achieved using 250 ng/ml α factor for YPL cultures (lower concentrations resulted in incomplete arrest, data not shown) and 50 ng/ml α factor for YPD cultures. For G2/M cell cycle arrest, 1% DMSO and 20 μg/ml nocodazole were added. Cultures were allowed to arrest for 1.5 generation times prior to DSB induction. (Un)budded cell fractions were determined by visually scoring at least 200 cells per sample. To induce DSB formation, 2% galactose and 2 μM β-estradiol (diluted from a stock solution of 10 mM β-estradiol in 100% ethanol) were added to *GAL-HO* cells and *lexO-HO* cells, respectively. We withdrew ca. $10^8$ cells per sample, added 0.1% sodium azide, collected cells by centrifugation, washed with TE (10 mM Tris, 1 mM EDTA, pH 8) containing 0.1% sodium azide, and stored cell pellets at −20°C.

We extracted genomic DNA using the MasterPure™ Yeast DNA Purification Kit (Lucigen), including RNase treatment, and quantified DNA concentrations using the QuantiFluor® dsDNA System (Promega) according to the manufacturers' instructions.

Genomic DNA was diluted in CutSmart® buffer (New England Biolabs) and analyzed by qPCR. Per sample triplicates containing 13 ng genomic DNA, 300 nM of each forward and reverse primer, and 1× SsoAdvanced™ Universal SYBR® Green Supermix (Biorad) in a total volume of 10 μl were prepared and run on a CFX384™ Real-Time System (Biorad) with 10 min initial denaturation at 95°C, followed by 40 cycles of 10 sec denaturation at 95°C and 1 min annealing and extension at 58°C. Primers used are listed in Supplementary Table S4. The fraction of cut genomes $f$ was calculated according to (35) as

$$f = 1 - \frac{(E_{DSB})^{\Delta C_q(t_0-t)}}{(E_{ADH1})^{\Delta C_q(t_0-t)}}$$

where $E_{DSB}$ and $E_{ADH1}$ are the primer efficiencies for the amplicon spanning the DSB formation site and the *ADH1* reference amplicon, respectively, and $\Delta C_q(t_0 - t)$ is the difference between the quantification cycles at the initial time point (prior to DSB induction) and the evaluated time point.

### Single strand annealing (SSA) assay

Cells with the SSA cassette and with *lexO-HO* or *GAL-HO* were grown in SD-His and SR-His, respectively, to suppress accumulation of $His^-$ recombinants prior to the beginning of the experiments.

To evaluate HO-induced recombination efficiency, *lexO-HO* cells were spread on YPD plates with or without 2 μM β-estradiol and *GAL-HO* cells were spread on YPG plates or YPD plates. After 2 days of growth, the survival frequency was calculated as the number of colonies growing on inducing media divided by the number of colonies growing on non-inducing media. Recombination was confirmed by replica-plating on selective media lacking uracil or histidine.

To evaluate leaky HO expression in the absence of inducers, cells were grown in media lacking histidine to suppress accumulation of $His^-$ recombinants prior to the beginning of the experiments. Then *GAL-HO* cells were transferred to YPR and *lexO-HO* cells to YPD and kept in the exponential growth phase by serial dilution. Prior and four days after the media change, cells were spotted in a 1:10 dilution series on YPD and SD-Ura plates and grown for 2 days. Colonies appearing on the SD-Ura plates were restruck on SD-His plates to confirm loss of histidine prototrophy.

To evaluate HO-independent spontaneous recombination, strains containing the SSA cassette but lacking the HO genes were used in all assays.

### Pulse field gel electrophoresis

Cells containing the *lexO-AscI* or *lexO-SrfI* system were grown in YPD and arrested in G2/M by addition of 1% DMSO and 20 μg/ml Nocodazole for 1.5 generation times. DSB formation was induced by addition of 2 μM β-estradiol. Per sample, we withdrew ca. $5.5 \times 10^8$ cells, added 0.1% sodium azide, collected cells by centrifugation, washed with TE containing 0.1% sodium azide, and stored cell pellets at −20°C. Pellets were washed in 100 mM EDTA pH 8. Per mg cell pellet, we added 0.4 μl 25 mg/ml Zymolyase 20T in 10 mM $KPO_4$ pH 7.5, 4.5 μl 100 mM EDTA pH 8, and 4.5 μl molten 1% Certified™ Low Melt Agarose (Biorad) in 100 mM EDTA pH 8. The pellet weight of the first

time point sample was assumed for all subsequent samples and the increased true pellet weight (due to cell growth without cell division) was compensated by reducing the amount of added 100 mM EDTA pH 8. The suspension was mixed and filled into plug molds (Biorad). After solidification, the plugs were incubated in 500 mM EDTA and 10 mM Tris pH 8 overnight at 37°C. We then added 1.4% sarcosyl and 1.4 mg/ml proteinase K and incubated the plugs overnight at 50°C. Plugs were washed four times in TE for 1 h at room temperature. For the *in vitro* digest, plugs were subsequently equilibrated four times in CutSmart® buffer (New England Biolabs) for 1 h at room temperature. Plugs were then incubated in 250 μl CutSmart® buffer containing 100 U commercial enzyme (New England Biolabs) at 4°C overnight followed by incubation at 37°C overnight and four 1 h washes in TE at room temperature. Plug slices were embedded into pulse field gels (1% Pulse Field Certified Agarose [Biorad] in 0.5× TBE [Biorad]) and run in 0.5× TBE (Biorad) on a CHEF-DR® II system (Biorad) for 66 h at 14°C and 5 V/cm with an initial switch time of 47 s and a final switch time of 170 s. The gel was stained with 1× SYBR™ Gold (Invitrogen) in 0.5× TBE (50 mM Tris, 50 mM boric acid, 10 mM EDTA) for 1 h in the dark and imaged with a Gel Doc™ XR+ imager (Biorad).

### DSB induction sensitivity assay

Cells were grown in YPD or YPL to exponential growth and spotted on YPD or YPG medium with or without 2 μM β-estradiol. YPD and YPG plates were incubated for 2 and 3 days, respectively.

### Western blotting

Western blotting was performed according to standard procedures. Briefly, protein extracts were prepared from 10 ml samples with $OD_{600\,nm} \approx 1$ as described previously (36). 10 μl protein extracts were run on 10% polyacrylamide gels using the Mini-PROTEAN system (Biorad), transferred on PVDF membranes using the iBlot™ 2 system, stained with Ponceau S solution, and blocked with 3% milk in TBS-T (20 mM Tris, 150 mM NaCl, 0.1% Tween 20, pH 7.5). FLAG tags were detected using anti-FLAG primary antibody (Sigma F1804, 1:2000 in TBS-T + 5% BSA + 0.05% $NaN_3$) and mouse IgGκ binding protein-HRP (Santa Cruz sc-516102, 1:5000 in TBS-T + 1% milk) and visualized using the SuperSignal™ West Femto Maximum Sensitivity Substrate (Thermo Scientific) and the Amersham™ Imager 600.

### *In vitro* cutting assay

The repair templates for the *hocs::REcs* genome engineering (see above) were used as substrates for the *in vitro* cutting assay. Per reaction, 200 ng column-purified substrate were incubated for 2 h with varying amounts of restriction enzyme (New England Biolabs) in 10 μl CutSmart® (New England Biolabs) at 37°C or in 10 μl 'yeast cytosol-like buffer' ('YCB') containing 300 mM potassium, 20 mM sodium, 2 mM magnesium, 0.5 mM calcium, 2.5 mM sulfate, 50 mM phosphate, 245 glutamate, and 0.1 mg/ml BSA, pH 6.8 (37) at 30°C. The reactions were then mixed with 6× Gel Loading Dye Purple (New England Biolabs), run on 2% agarose gels containing 0.00005% ethidium bromide in 0.5× TBE, and imaged.

### Data analysis and visualization

All data analysis and visualization was done with the statistical software R (version 3.6.2) using custom scripts (available upon request). We used the R packages Biostrings (version 2.52.0) and BSgenome.Scerevisiae.UCSC.sacCer3 (version 1.4.0) for the localization of restriction enzyme recognition sites in the *S. cerevisiae* genome. We used the R package Gviz (version 1.28.3) (38) to plot the MNase-seq data from (39) around genomic AscI and SrfI sites.

### Reagent Availability

All yeast strains are available upon request. Plasmids are available from Addgene or upon request (see Supplementary Table S1).

## RESULTS

### The *lexO-HO* DSB formation system is fast, efficient, and growth media-independent

To overcome the media requirements of the *GAL-HO* system and the associated slow cell growth, we employed a heterologous induction system (30). This system is based on an engineered transcription factor, which is a fusion comprised of the bacterial DNA-binding protein LexA, an estrogen receptor domain, and the bacteria-derived transactivation domain B112. The transcription factor is constitutively expressed, but translocates into the nucleus only in the presence of estrogen hormones. It then binds to an engineered promoter consisting of LexA binding sites fused to the yeast *CYC1* core promoter ($P_{lexO}$) to drive target gene expression. We combined, both, the transcription factor and the $P_{lexO}$-*HO* gene, hereafter called the *lexO-HO* system, in the same integrative yeast plasmid with the *LEU2MX* selection marker (Supplementary Figure S1A). To increase compatibility with various strain backgrounds, we also cloned versions with the *URA3MX* or *HIS3MX* selection marker (Supplementary Table S1).

To evaluate DSB formation with *lexO-HO*, we used a yeast strain that contained the natural HO target site at the *MAT* locus, but lacked the *HML* and *HMR* repair cassettes to create an unrepairable DSB (Figure 1A). We grew the strain in complex yeast media containing glucose (YPD), which allows for optimal growth, and induced HO expression by adding the estrogen hormone β-estradiol. We monitored DSB formation by quantitative PCR (qPCR) and found fast and efficient cutting (Figure 1B). More than 70% of the target sites were cut 0.5 h after hormone addition and complete cutting was achieved after about 1 h. For a comparison, we also monitored target site cutting in a *GAL-HO* containing strain and found similar cutting kinetics upon galactose induction. As expected, continuous *lexO-HO* induction reduced cell viability considerably and to the same extent as *GAL-HO* induction (Supplementary Figure S2). Additionally, β-estradiol was stable in YPD medium at 30°C for at least seven days (Supplementary Figure S3). We

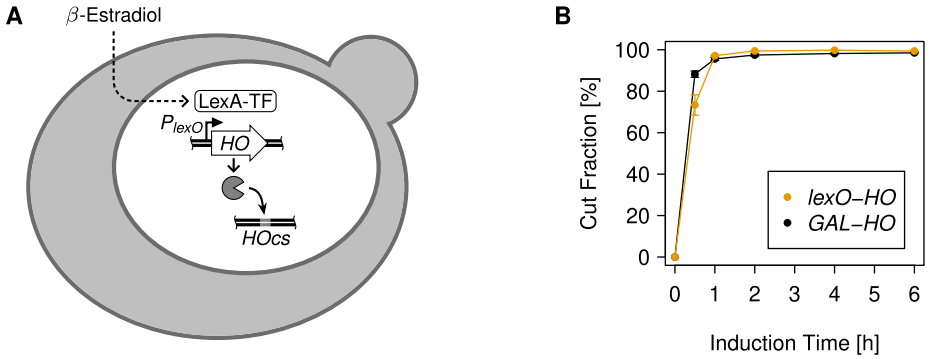


**Figure 1.** DSB formation with the *lexO-HO* system is fast and efficient. (**A**) Schematic of the *lexO-HO* system. An unrepairable DSB is generated at the *MAT* HO cut site (*HOcs*), as the repair templates *HML* and *HMR* are deleted (not shown). (**B**) DSB formation upon induction of the *lexO-HO* or *GAL-HO* system was evaluated by qPCR. Means ± standard deviations of three biological replicates are plotted.

conclude that the *lexO-HO* system enables robust, fast, and efficient DSB formation.

To test if the *lexO-HO* system allowed DSB formation in a growth media-independent fashion, we induced HO expression in complex yeast media containing glucose (YPD), lactic acid (YPL), or lactic acid and galactose (YPLG), or in synthetic medium (SD). In YPD and SD, DSB formation was fast and we observed complete target site cutting within 1 h (Supplementary Figure S4). In YPL and YPLG, DSB formation was slower, but >80% of the target sites were cut within 2 h. We conclude that DSBs can be generated with *lexO-HO* in various growth media, although the kinetics may differ.

DSB repair pathway choice depends on the cell cycle stage (40) and, thus, DSB formation in synchronized cell populations is desirable in some experimental settings. To test if the *lexO-HO* system can generate DSBs in different cell cycle stages, we induced it in G1 or G2/M-arrested cells. In G1-arrested cells, DSB formation was slower and incomplete in contrast to cycling cells, but reached about 70% cut target sites within 1 h (Supplementary Figure S5A). We observed that also *GAL-HO*-mediated DSB formation was slowed down and incomplete (80%) in G1-arrested cells. In G2/M arrested cells, both, *lexO-HO* and *GAL-HO*-mediated DSB formation was fast and complete within 1 h (Supplementary Figure S5B). Thus, *lexO-HO* facilitates DSB formation in cell-cycle arrested cells, although cleavage is incomplete in G1-arrested cells.

### Leaky DSB formation is low when the *lexO-HO* system is not induced

An essential requirement for any DSB formation system is low expression in the absence of the inducer (leakiness) to prevent unscheduled DSBs. To evaluate the leakiness of the *lexO-HO* system, we devised a single strand annealing (SSA) assay (Figure 2A). We split the *URA3MX* gene into two overlapping parts and inserted the 5′ part upstream and the 3′ part downstream of the HO cut site at the *MAT* locus. We placed a *HIS3MX* marker gene between the HO cut site and the *URA3MX* 3′ part. DSB formation at the HO cut site, resection of the DSB ends, and annealing of the overlapping *URA3MX* sequences will form a functional *URA3MX* gene and remove the *HIS3MX* gene. To confirm the validity of the assay system, we induced HO expression and found more than 95% surviving cells and the expected switch of histidine to uracil prototrophy (Figure 2B). We then grew cells with the SSA cassette and *lexO-HO* under non-inducing conditions (YPD without β-estradiol) for four days and evaluated cassette recombination by spot assay on selective media lacking uracil (Figure 2C). We found negligible cassette recombination. As a comparison, with non-induced *GAL-HO* (grown in YP with raffinose and without galactose) we detected a slightly higher cassette recombination. As expected, all $Ura^+$ recombinants had lost the *HIS3MX* marker and did not grow when restruck on media lacking histidine (data not shown). We conclude that leaky DSB formation is low when the *lexO-HO* system is not induced.

### Expression of bacterial restriction enzymes generates DSBs in live yeast cells

We sought a system to create a few dozen defined and unique DSBs in the *S. cerevisiae* genome. We found that the restriction enzymes AsiSI, AscI, FseI, SbfI, and SrfI have 38, 28, 22, 96, and 20 naturally occurring 8 bp recognition sites in the yeast genome (S288C), respectively (Supplementary Figure S6). The recognition sequences do not occur in mitochondrial DNA, yeast transposons, ribosomal DNA, telomeric and subtelomeric repeats, or the 2 micron plasmid. We cloned yeast codon usage-optimized genes encoding these restriction enzymes, added a nuclear localization sequence, and controlled their expression in yeast cells with the *lexO* system (Figure 3A and Supplementary Figure S1B).

To compare how efficiently the different restriction enzymes could generate DSBs, we inserted their recognition sequence at the *MAT* HO cleavage site and monitored cutting by qPCR. We found that SrfI cutting was comparable to cutting with HO (Figure 3B). AscI led to complete cutting within 2 h of induction. SbfI, FseI, and AsiSI cut with slower kinetics. As expected, restriction enzyme expression also considerably reduced cell viability (Figure 3C). We conclude that the bacterial restriction enzymes AsiSI, AscI, FseI, SbfI, and SrfI can be used to create DSBs in live yeast cells and that SrfI and AscI allow DSB formation with fast kinetics.

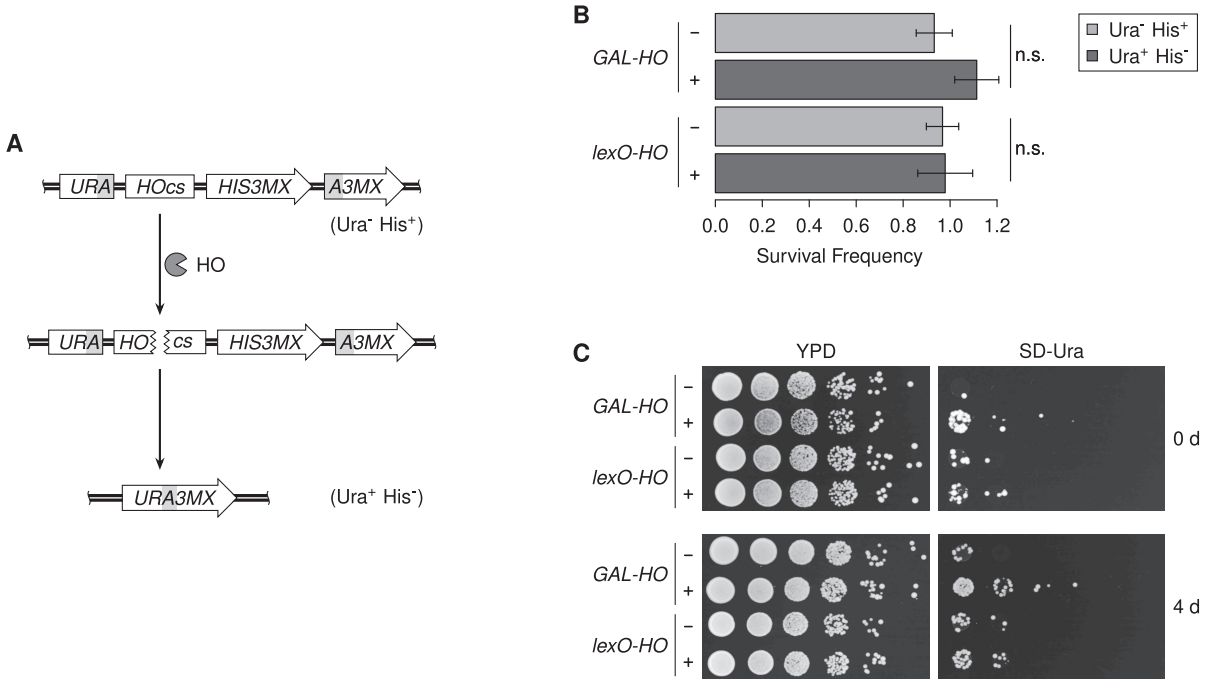


**Figure 2.** Leaky DSB formation is low when *lexO-HO* is not induced. (**A**) Schematic of the single strand annealing (SSA) assay. Repair of the HO-induced DSB by SSA results in the formation of an intact *URA3MX* gene, while the *HIS3MX* gene is lost. (**B**) HO induction results in efficient recombination of the SSA cassette. Cells with the SSA cassette and with (+) or without (–) the indicated *HO* genes were grown on inducing and non-inducing media and survival frequencies were calculated by dividing the number of colonies forming under these conditions. Histidine and uracil prototrophy of colonies grown on inducing media was evaluated by replica-plating on selective media. The mean ± standard deviation of three biological replicates is plotted. n.s.: not significant (Student's *t*-test). (**C**) Evaluation of leaky HO expression. Strains with the SSA cassette and with (+) or without (–) the indicated *HO* genes were grown in non-inducing conditions for the indicated time and then spotted on the indicated media in a 1:10 dilution series. A representative example of three biological replicates is shown. See Materials and Methods for experimental details.

We considered two possibilities for the variation in cutting kinetics displayed by the restriction endonucleases: (i) different nuclease expression levels and (ii) different enzymatic activities in yeast cells. By western blot analysis we indeed found expression level differences. However, they did not correlate with the observed cutting kinetics (Supplementary Figure S7). To evaluate if the nucleases have different enzymatic activities inside *S. cerevisiae* cells, we tested the *in vitro* activities of SrfI, AscI, and AsiSI in a buffer reflecting the yeast interior milieu (37). We found high activity for SrfI, modest activity for AscI, and weak activity for AsiSI (Supplementary Figure S8). Thus, the different cutting kinetics are probably attributable to the nucleases' enzymatic activities in *S. cerevisiae* cells.

### Bacterial restriction enzyme expression generates multiple defined DSBs in the yeast genome

To evaluate DSB formation at the endogenous recognition sequences in the yeast genome, we used pulse field gel electrophoresis. The structure of S-phase chromosomes prevents them from entering the gel. To avoid this problem, we used G2-arrested cells. Upon SrfI induction, bands corresponding to intact chromosomes disappeared within 1 or 2 h, indicating that at least one of their SrfI recognition sites was cut (Figure 4A). By comparison with *in vitro* digested chromosomal DNA, several new bands could be identified as final cutting products. Some bands appeared transiently and most likely corresponded to intermediate products containing yet uncleaved SrfI recognition sites. We noted that the shorter cutting product bands shifted up over time indicating resection of their ends (41). Notably, the bands corresponding to chromosomes I, VI, VIII, and XI, which lack SrfI recognition sites, remained unchanged throughout the experiment. We obtained similar results when expressing AscI, albeit with slightly slower cutting kinetics (Supplementary Figure S9A). We conclude that SrfI or AscI expression leads to fast DSB formation exclusively at their recognition sites in the yeast genome.

We wondered if the cutting kinetics differed between specific sites and if there was an influence of the local chromatin structure. Using a published MNase-seq data set (39), we selected SrfI recognition sites located in regions of high or low nucleosome occupancy (Supplementary Figure S10) and quantified DSB formation at these sites by qPCR. Cutting kinetics indeed differed between some sites and were negatively correlated with nucleosome occupancy (Figure 4B). We found similar results for AscI (Supplementary Figure S9B). Importantly, most sites were completely cut within 4 h and all sites were cut within 8 h of induction. Thus, DSB formation at specific SrfI and AscI sites varies and is negatively influenced by nucleosome occupancy.

## DISCUSSION

The goal of this study was to develop growth media-independent, tightly regulated, and efficient systems to create DSBs at a unique site or multiple defined sites in the

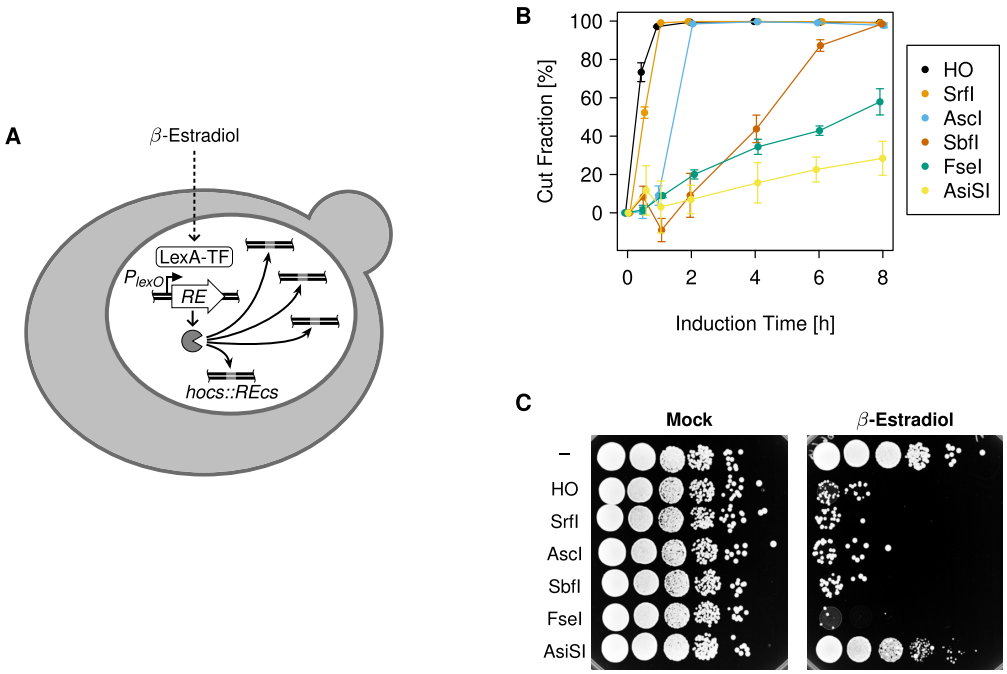


**Figure 3.** Expression of bacterial restriction enzymes generates DSBs in live yeast cells. (**A**) Schematic of restriction enzyme (RE)-mediated DSB formation in yeast. DSBs are created at the endogenous restriction sites and at an engineered *MAT* HO cut site (*hocs::REcs*). A DSB at *hocs::REcs* is unrepairable, as *HML* and *HMR* are deleted (not shown). (**B**) DSB formation at *hocs::REcs* upon induction of the *lexO-RE* systems was evaluated by qPCR. For a comparison, DSB formation with the *lexO-HO* system was measured as well. Means ± standard deviations of three biological replicates are plotted. (**C**) DSB induction sensitivity assay. Cells with the indicated endonucleases under the control of the *lexO* system were spotted in a 1:10 dilution series on media without or with β-estradiol. As a control, cells lacking an inducible nuclease gene were spotted as well (–). A representative example of three biological replicates is shown.

*S. cerevisiae* genome. We achieved this goal using an engineered induction system to control expression of the yeast endogenous HO endonuclease or bacterial restriction enzymes with ca. 20–100 endogenous recognition sites.

We developed the *lexO-HO* system to alleviate the media requirements of the *GAL-HO* system, which results in reduced cell growth and makes working with slow-growing mutant strains tedious. The *lexO-HO* system is based on the engineered induction system described in (30), which had been developed to be growth media-independent. Accordingly, *lexO-HO* facilitated DSB formation in various media. Specifically we could generate DSBs in media for optimal growth (YPD), in media that would allow e.g. galactose induction of other genes (YPL and YPLG), and in media for plasmid selection (SD). The media-independence of the *lexO-HO* system can be exploited to study how DSB signaling and repair may differ in various metabolic states. This could facilitate new insights into the interplay between the cell's metabolism and the DNA damage response, which has been implicated in cancer, aging, and metabolic diseases (42–45).

*lexO-HO* induction resulted in fast and efficient DSB formation in most tested conditions. We found reduced and slower DSB formation in G1-arrested cells, where the generation of DSBs is most likely counteracted by their efficient religation via the non-homologous end joining (NHEJ) pathway (46). The *lexO-HO* system might not reach a high enough HO expression level to push the DSB formation/religation equilibrium further. If complete DSB formation in G1-arrested cells is desired, the *lexO-HO* system could potentially be modified for higher HO expression levels for example by increasing its copy number. Alternatively, NHEJ factors could be deleted. *lexO-HO*-mediated DSB formation was also reduced in unsynchronized YPL and YPLG cultures. Compared to YPD medium, these media result in a slowed-down cell cycle progression and a prolonged G1 phase (47,48), where DSB formation probably competes with NHEJ-mediated religation. The HO expression level achieved with *lexO-HO* seems not to be high enough to sustain fast DSB formation in this situation. In contrast, efficient DSB formation could be achieved with *GAL-HO* under these conditions, suggesting that HO expression using the *GAL10* promoter is stronger than with the *lexO* system.

Using an SSA assay as a readout, we found leakiness of the *lexO-HO* system to be low. This prevents unscheduled DSB formation and associated problems, such as target site mutations, which would prevent further DSB formation, and premature product formation in recombination assays. Thus, the *lexO-HO* system could be used in a variety of DSB repair assays.

One limitation of the *lexO-HO* system is that HO expression cannot be easily shut off for transient DSB formation. In contrast, the *GAL-HO* system can be transcriptionally repressed by glucose addition to the culture media (15). To achieve transient HO expression with the *lexO-HO* system, the anchor-away system (49) or the auxin-inducible degradation system (50) could be used, although, given the al-

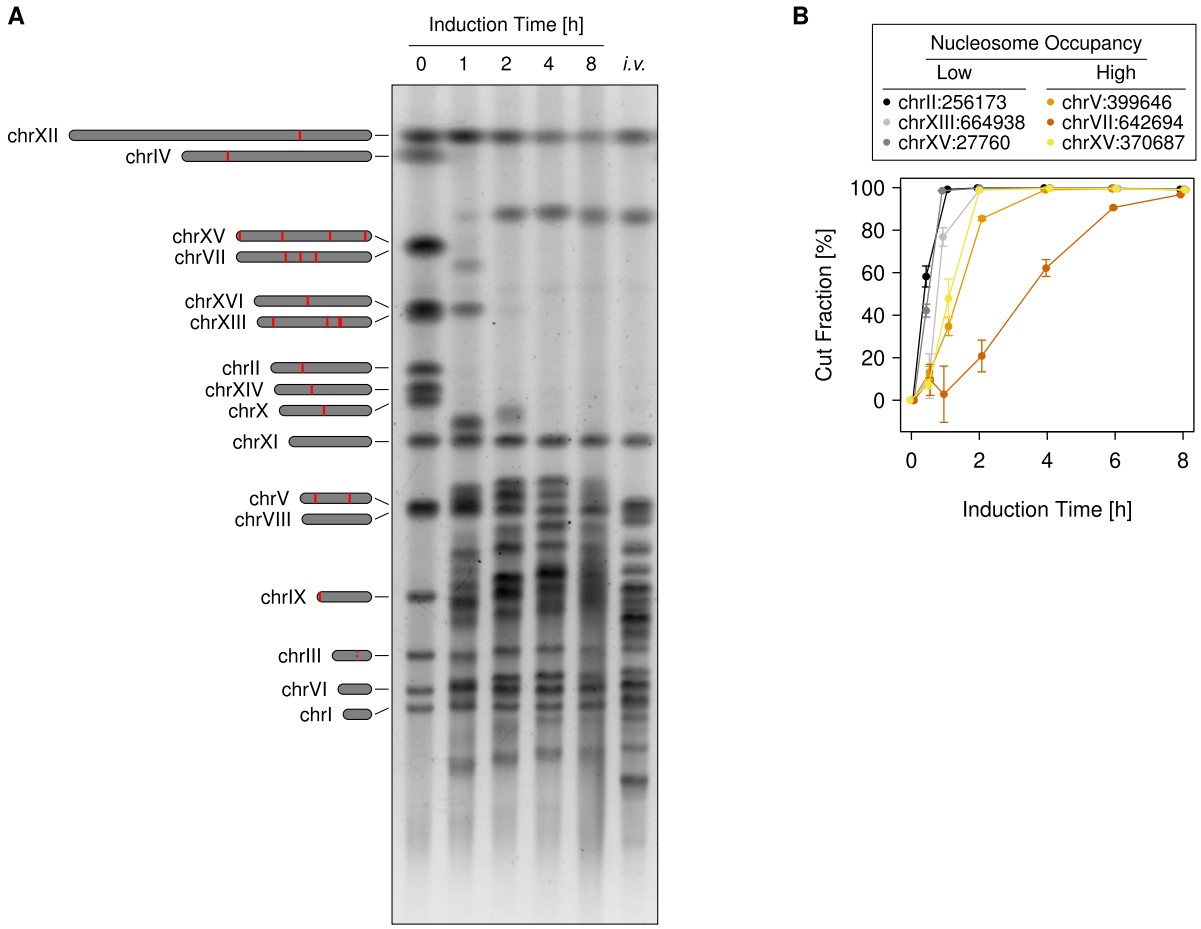


**Figure 4.** Multiple DSB generation with *lexO-SrfI*. (**A**) Pulse field gel electrophoresis of cleaved chromosomes upon SrfI induction. On the left, chromosomes are drawn to scale and SrfI recognition site locations are indicated by red lines. The SrfI site on chrIII was engineered into the *MAT* HO cut site (dashed red line). *i.v.*: *in vitro* digest of the 0 h sample with commercial SrfI (NEB). A representative example of two biological replicates is shown. (**B**) DSB formation at genomic SrfI recognition sites was evaluated by qPCR. Means ± standard deviations of three biological replicates are plotted. Nucleosome occupancy was evaluated using MNase-seq data from (39). See also Supplementary Figure S10.

ready short HO half-life (51), success might be limited for the latter approach. In DSB repair-proficient strains, the *lexO-HO* system could also be flanked with HO cut sites and possibly direct repeats to remove its genes by SSA upon induction (52).

Another goal of this study was to devise a system for the inducible formation of multiple defined DSBs in the yeast genome. To this end, we expressed the bacterial restriction enzymes AscI, AsiSI, FseI, SbfI, or SrfI, whose 8 bp recognition sequences naturally occur at ca. 20–100 sites in the yeast genome. We found that all five tested restriction enzymes could cut genomic DNA in live yeast cells. SrfI and AscI showed the fastest cutting at an engineered recognition sequence within the *MAT* HO cut site. Cutting kinetics differed among the other genomic recognition sites, where high nucleosome occupancy was correlated with less efficient cutting. This observation parallels the finding that Cas9-mediated cleavage efficiency is reduced in regions of high nucleosome occupancy (53).

Interestingly, AsiSI cut with the slowest kinetics in live yeast cells. AsiSI has been used for DSB formation in mammalian cells, where it shows fast cutting at some genomic sites (54). A reason for this difference might be that we added an NLS and FLAG tag at AsiSI's C terminus, while AsiSI is tagged N-terminally in the mammalian system. Independently of the tagging, AsiSI's enzymatic activity might be poor in the yeast interior milieu. Supporting this notion we found poor activity of AsiSI in a corresponding *in vitro* assay.

The employed restriction enzymes generate different DSB ends. AscI generates ends with 4 nt 5′ overhangs, AsiSI generates 2 nt 3′ overhangs, SrfI generates blunt ends, and FseI and SbfI generate 4 nt 3′ overhangs. Various DSB processing enzymes show different activities for substrates with blunt ends, 3′ overhangs, or 5′ overhangs *in vitro* (55,56). The restriction enzyme systems presented here can be used to confirm and extend these observations *in vivo*.

We envision that our system can be coupled with high-throughput technologies to elucidate the impact of chromatin context on DSB processing. Indeed, multi DSB formation systems in mammalian cells based on I-PpoI or AsiSI in combination with ChIP-chip or ChIP-seq revealed the interplay between repair factor recruitment, chromatin modifications, and transcription at DSBs (54,57–59). One

advantage of our yeast system is that DSB formation is fast and complete at most evaluated sites, which will result in temporally homogeneous DSB processing in a cell population, supporting quantitative analysis of DSB repair events. To direct DSB formation to specific genome regions of interest, further recognition sequences can be added by CRISPR/Cas9-mediated genome engineering. In the case of AscI, new cleavage sites can also be easily inserted using the dominant marker cassettes that are commonly used for PCR-mediated gene knock-outs in *S. cerevisiae*, as these cassettes usually contain an AscI site (33,60). Sites of low nucleosome occupancy should be chosen to achieve fast and efficient cutting.

Finally, the *lexO*-based induction system could also be used to control the expression of other endonucleases, such as Cas9 or I-SceI. I-SceI is a yeast-endogenous endonuclease encoded within a self-splicing intron in the mitochondrial rDNA locus (61). I-SceI creates a DSB in intron-less rDNA loci to stimulate recombination and spreading of its gene in a gene drive-like process called intron homing. Inducible I-SceI expression has been used for site-specific DSB formation in both yeast and mammalian cells (62,63).

In summary, our systems for the formation of single or multiple defined DSBs in the yeast genome are fast, efficient, and growth media-independent. We expect that they will prove to be useful tools for DSB repair studies in *S. cerevisiae*.

## SUPPLEMENTARY DATA

Supplementary Data are available at NAR Online.

## ACKNOWLEDGEMENTS

We thank New England Biolabs for providing the SrfI protein sequence; members of the Symington laboratory for discussions; and W.K. Holloman, M.T. Kimble, L. Marie, and D.S.M. Ottoz for critical reading of and thoughtful comments on the manuscript.

## FUNDING

National Institutes of Health [GM126997 to L.S.S.]. Funding for open access charge: National Institutes of Health (National Institute of General Medical Sciences) [GM126997].
*Conflict of interest statement.* None declared.

## REFERENCES

1. Hoeijmakers,J.H.J. (2009) DNA damage, aging, and cancer. *New Engl. J. Med.*, **361**, 1475–1485.
2. Mehta,A. and Haber,J.E. (2014) Sources of DNA double-strand breaks and models of recombinational DNA repair. *CSH Perspect. Biol.*, **6**, a016428.
3. Lam,I. and Keeney,S. (2014) Mechanism and regulation of meiotic recombination initiation. *CSH Perspect. Biol.*, **7**, a016634.
4. Chi,X., Li,Y. and Qiu,X. (2020) V(D)J recombination, somatic hypermutation and class switch recombination of immunoglobulins: mechanism and regulation. *Immunology*, **160**, 233–247.
5. Maeder,M.L. and Gersbach,C.A. (2016) Genome-editing technologies for gene and cell therapy. *Mol. Ther.*, **24**, 430–446.
6. Kowalczykowski,S.C. (2015) An overview of the molecular mechanisms of recombinational DNA repair. *CSH Perspect. Biol.*, **7**, a016410.
7. O'Driscoll,M. (2012) Diseases associated with defective responses to DNA damage. *CSH Perspect. Biol.*, **4**, a012773.
8. Pâques,F., Leung,W.Y. and Haber,J.E. (1998) Expansions and contractions in a tandem repeat induced by double-strand break repair. *Mol. Cell Biol.*, **18**, 2045–2054.
9. Connolly,B., White,C.I. and Haber,J.E. (1988) Physical monitoring of mating type switching in *Saccharomyces cerevisiae*. *Mol. Cell Biol.*, **8**, 2342–2349.
10. Miné-Hattab,J. and Rothstein,R. (2012) Increased chromosome mobility facilitates homology search during recombination. *Nat. Cell Biol.*, **14**, 510–517.
11. Pierce,A.J., Johnson,R.D., Thompson,L.H. and Jasin,M. (1999) XRCC3 promotes homology-directed repair of DNA damage in mammalian cells. *Gene. Dev.*, **13**, 2633–2638.
12. Sugawara,N., Wang,X. and Haber,J.E. (2003) In vivo roles of Rad52, Rad54, and Rad55 proteins in Rad51-mediated recombination. *Mol. Cell*, **12**, 209–219.
13. Haber,J.E. (2012) Mating-type genes and MAT switching in *Saccharomyces cerevisiae*. *Genetics*, **191**, 33–64.
14. Herskowitz,I. and Jensen,R.E. (1991) Putting the HO gene to work: practical uses for mating-type switching. *Method Enzymol.*, **194**, 132–146.
15. Johnston,M. (1987) A model fungal gene regulatory mechanism: the GAL genes of *Saccharomyces cerevisiae*. *Microbiol. Rev.*, **51**, 458–476.
16. Hovland,P., Flick,J., Johnston,M. and Sclafani,R.A. (1989) Galactose as a gratuitous inducer of GAL gene expression in yeasts growing on glucose. *Gene*, **83**, 57–64.
17. Frederick,D.L. and Tatchell,K. (1996) The REG2 gene of *Saccharomyces cerevisiae* encodes a type 1 protein phosphatase-binding protein that functions with Reg1p and the Snf1 protein kinase to regulate growth. *Mol. Cell Biol.*, **16**, 2922–2931.
18. Uesono,Y., Ashe,M.P. and Toh-E,A. (2004) Simultaneous yet independent regulation of actin cytoskeletal organization and translation initiation by glucose in *Saccharomyces cerevisiae*. *Mol. Biol. Cell*, **15**, 1544–1556.
19. Kondo,T., Wakayama,T., Naiki,T., Matsumoto,K. and Sugimoto,K. (2001) Recruitment of Mec1 and Ddc1 checkpoint proteins to double-strand breaks through distinct mechanisms. *Science*, **294**, 867–870.
20. Wolner,B., van Komen,S., Sung,P. and Peterson,C.L. (2003) Recruitment of the recombinational repair machinery to a DNA double-strand break in yeast. *Mol. Cell*, **12**, 221–232.
21. Miyazaki,T., Bressan,D.A., Shinohara,M., Haber,J.E. and Shinohara,A. (2004) In vivo assembly and disassembly of Rad51 and Rad52 complexes during double-strand break repair. *EMBO J.*, **23**, 939–949.
22. Gartenberg,M.R. and Smith,J.S. (2016) The nuts and bolts of transcriptionally silent chromatin in *Saccharomyces cerevisiae*. *Genetics*, **203**, 1563–1599.
23. Nickoloff,J.A., Chen,E.Y. and Heffron,F. (1986) A 24-base-pair DNA sequence from the MAT locus stimulates intergenic recombination in yeast. *Proc. Natl. Acad. Sci. U.S.A.*, **83**, 7831–7835.
24. Llorente,B. and Symington,L.S. (2004) The Mre11 nuclease is not required for 5′ to 3′ resection at multiple HO-induced double-strand breaks. *Mol. Cell Biol.*, **24**, 9682–9694.
25. Lewis,L.K., Kirchner,J.M. and Resnick,M.A. (1998) Requirement for end-joining and checkpoint functions, but not RAD52-mediated recombination, after EcoRI endonuclease cleavage of *Saccharomyces cerevisiae* DNA. *Mol. Cell Biol.*, **18**, 1891–1902.
26. Lewis,L.K., Westmoreland,J.W. and Resnick,M.A. (1999) Repair of endonuclease-induced double-strand breaks in *Saccharomyces cerevisiae*: essential role for genes associated with nonhomologous end-joining. *Genetics*, **152**, 1513–1529.
27. Westmoreland,J.W., Summers,J.A., Holland,C.L., Resnick,M.A. and Lewis,L.K. (2010) Blunt-ended DNA double-strand breaks induced by endonucleases PvuII and EcoRV are poor substrates for repair in *Saccharomyces cerevisiae*. *DNA Repair*, **9**, 617–626.
28. Gnügge,R., Liphardt,T. and Rudolf,F. (2016) A shuttle vector series for precise genetic engineering of *Saccharomyces cerevisiae*. *Yeast*, **33**, 83–98.

29. Diede,S.J. and Gottschling,D.E. (1999) Telomerase-mediated telomere addition in vivo requires DNA primase and DNA polymerases alpha and delta. *Cell*, **99**, 723–733.
30. Ottoz,D. S.M., Rudolf,F. and Stelling,J. (2014) Inducible, tightly regulated and growth condition-independent transcription factor in *Saccharomyces cerevisiae*. *Nucleic Acids Res.*, **42**, e130.
31. Ryan,O.W., Skerker,J.M., Maurer,M.J., Li,X., Tsai,J.C., Poddar,S., Lee,M.E., DeLoache,W., Dueber,J.E., Arkin,A.P. *et al.* (2014) Selection of chromosomal DNA libraries using a multiplex CRISPR system. *eLife*, **3**, e03703.
32. Gietz,R.D. and Woods,R.A. (2002) Transformation of yeast by lithium acetate/single-stranded carrier DNA/polyethylene glycol method. *Method Enzymol.*, **350**, 87–96.
33. Goldstein,A.L. and McCusker,J.H. (1999) Three new dominant drug resistance cassettes for gene disruption in *Saccharomyces cerevisiae*. *Yeast*, **15**, 1541–1553.
34. Gnügge,R., Oh,J. and Symington,L.S. (2018) Processing of DNA double-dtrand breaks in yeast. *Method Enzymol.*, **600**, 1–24.
35. Pfaffl,M.W. (2001) A new mathematical model for relative quantification in real-time RT-PCR. *Nucleic Acids Res.*, **29**, e45.
36. Carpenter,K., Bell,R.B., Yunus,J., Amon,A. and Berchowitz,L.E. (2018) Phosphorylation-mediated clearance of amyloid-like assemblies in meiosis. *Dev. Cell*, **45**, 392–405.
37. van Eunen,K., Bouwman,J., Daran-Lapujade,P., Postmus,J., Canelas,A.B., Mensonides,F.I.C., Orij,R., Tuzun,I., van den Brink,J., Smits,G.J. *et al.* (2010) Measuring enzyme activities under standardized in vivo-like conditions for systems biology. *FEBS J.*, **277**, 749–760.
38. Hahne,F. and Ivanek,R. (2016) Visualizing Genomic Data Using Gviz and Bioconductor. *Methods Mol. Biol.*, **1418**, 335–351.
39. Kubik,S., O'Duibhir,E., de Jonge,W.J., Mattarocci,S., Albert,B., Falcone,J.-L., Bruzzone,M.J., Holstege,F.C.P. and Shore,D. (2018) Sequence-directed action of RSC remodeler and general regulatory factors modulates +1 nucleosome position to facilitate transcription. *Mol. Cell*, **71**, 89–102.
40. Symington,L.S. and Gautier,J. (2011) Double-strand break end resection and repair pathway choice. *Annu. Rev. Genet.*, **45**, 247–271.
41. Westmoreland,J., Ma,W., Yan,Y., Van Hulle,K., Malkova,A. and Resnick,M.A. (2009) RAD50 is required for efficient initiation of resection and recombinational repair at random, gamma-induced double-strand break ends. *PLoS Genet.*, **5**, e1000656.
42. Turgeon,M.-O., Perry,N. J.S. and Poulogiannis,G. (2018) DNA damage, repair, and cancer metabolism. *Front. Ooncol.*, **8**, 15.
43. Li,H., Mitchell,J.R. and Hasty,P. (2008) DNA double-strand breaks: a potential causative factor for mammalian aging? *Mech. Ageing Dev.*, **129**, 416–424.
44. Shimizu,I., Yoshida,Y., Suda,M. and Minamino,T. (2014) DNA damage response and metabolic disease. *Cell Metab.*, **20**, 967–977.
45. Corcoles-Saez,I., Ferat,J.-L., Costanzo,M., Boone,C.M. and Cha,R.S. (2019) Functional link between mitochondria and Rnr3, the minor catalytic subunit of yeast ribonucleotide reductase. *Microb. Cell*, **6**, 286–294.
46. Chiruvella,K.K., Liang,Z. and Wilson,T.E. (2013) Repair of double-strand breaks by end joining. *CSH Perspect. Biol.*, **5**, a012757.
47. Silljé,H.H., ter Schure,E.G., Rommens,A.J., Huls,P.G., Woldringh,C.L., Verkleij,A.J., Boonstra,J. and Verrips,C.T. (1997) Effects of different carbon fluxes on G1 phase duration, cyclin expression, and reserve carbohydrate metabolism in *Saccharomyces cerevisiae*. *J. Bacteriol.*, **179**, 6560–6565.
48. Leitao,R.M. and Kellogg,D.R. (2017) The duration of mitosis and daughter cell size are modulated by nutrients in budding yeast. *J. Cell Biol.*, **216**, 3463–3470.
49. Haruki,H., Nishikawa,J. and Laemmli,U.K. (2008) The anchor-away technique: rapid, conditional establishment of yeast mutant phenotypes. *Mol. Cell*, **31**, 925–932.
50. Nishimura,K., Fukagawa,T., Takisawa,H., Kakimoto,T. and Kanemaki,M. (2009) An auxin-based degron system for the rapid depletion of proteins in nonplant cells. *Nat. Methods*, **6**, 917–922.
51. Kaplun,L., Ivantsiv,Y., Bakhrat,A. and Raveh,D. (2003) DNA damage response-mediated degradation of Ho endonuclease via the ubiquitin system involves its nuclear export. *J. Biol. Chem.*, **278**, 48727–48734.
52. Karathanasis,E. and Wilson,T.E. (2002) Enhancement of *Saccharomyces cerevisiae* end-joining efficiency by cell growth stage but not by impairment of recombination. *Genetics*, **161**, 1015–1027.
53. Yarrington,R.M., Verma,S., Schwartz,S., Trautman,J.K. and Carroll,D. (2018) Nucleosomes inhibit target cleavage by CRISPR-Cas9 in vivo. *Proc. Natl. Acad. Sci. U.S.A.*, **115**, 9351–9358.
54. Iacovoni,J.S., Caron,P., Lassadi,I., Nicolas,E., Massip,L., Trouche,D. and Legube,G. (2010) High-resolution profiling of gammaH2AX around DNA double strand breaks in the mammalian genome. *EMBO J.*, **29**, 1446–1457.
55. Paull,T.T. and Gellert,M. (1998) The 3′ to 5′ exonuclease activity of Mre 11 facilitates repair of DNA double-strand breaks. *Mol. Cell*, **1**, 969–979.
56. Cannavo,E., Cejka,P. and Kowalczykowski,S.C. (2013) Relationship of DNA degradation by *Saccharomyces cerevisiae* exonuclease 1 and its stimulation by RPA and Mre11-Rad50-Xrs2 to DNA end resection. *Proc. Natl. Acad. Sci. U.S.A.*, **110**, E1661–E1668.
57. Berkovich,E., Monnat,R.J. and Kastan,M.B. (2007) Roles of ATM and NBS1 in chromatin structure modulation and DNA double-strand break repair. *Nat. Cell Biol.*, **9**, 683–690.
58. Aymard,F., Bugler,B., Schmidt,C.K., Guillou,E., Caron,P., Briois,S., Iacovoni,J.S., Daburon,V., Miller,K.M., Jackson,S.P. *et al.* (2014) Transcriptionally active chromatin recruits homologous recombination at DNA double-strand breaks. *Nat. Struct. Mol. Biol.*, **21**, 366–374.
59. Clouaire,T., Rocher,V., Lashgari,A., Arnould,C., Aguirrebengoa,M., Biernacka,A., Skrzypczak,M., Aymard,F., Fongang,B., Dojer,N. *et al.* (2018) Comprehensive mapping of histone modifications at DNA double-strand breaks deciphers repair pathway chromatin signatures. *Mol. Cell*, **72**, 250–262.
60. Wach,A., Brachat,A., Pöhlmann,R. and Philippsen,P. (1994) New heterologous modules for classical or PCR-based gene disruptions in *Saccharomyces cerevisiae*. *Yeast*, **10**, 1793–1808.
61. Jacquier,A. and Dujon,B. (1985) An intron-encoded protein is active in a gene conversion process that spreads an intron into a mitochondrial gene. *Cell*, **41**, 383–394.
62. Plessis,A., Perrin,A., Haber,J.E. and Dujon,B. (1992) Site-specific recombination determined by I-SceI, a mitochondrial group I intron-encoded endonuclease expressed in the yeast nucleus. *Genetics*, **130**, 451–460.
63. Rouet,P., Smih,F. and Jasin,M. (1994) Introduction of double-strand breaks into the genome of mouse cells by expression of a rare-cutting endonuclease. *Mol. Cell Biol.*, **14**, 8096–8106.